Robust Design of Cascade Control

Claudio Maffezzoni, Nicola Schiavoni, and Gianni Ferretti

ABSTRACT: This paper presents a new design concept for cascade control that ensures enhanced robustness by minimizing the mutual influence among the cascaded loops. The practical impact of the new robust design is illustrated with both analytic and numerical examples.

Introduction

Cascade control is one of the most popular structures for process control [1]. In general, it is applied when the process can be split into two (or more) cascaded parts by measuring one (or more) intermediate variable(s) for the inner loop(s). The classical structure of a cascade control with two loops is shown in Fig. 1, where $H(s)$ and $G(s)$ are the transfer functions for the process subsystems and $R_1(s)$ and $R_2(s)$ are the corresponding transfer functions for the controllers. The usual approach to cascade control is to design the individual controllers sequentially, starting from the inner loop, and then taking into account the resulting inner closed-loop transfer function, designated $F_1(s)$ in Fig. 1, while synthesizing the outer loop.

Cascade controllers usually are designed to ensure a definite separation of the different loops in the frequency domain. This separation, in turn, allows independent design of the controllers and minimum interaction among the loops. However, there are a number of practical cases where the standard configuration of Fig. 1 cannot deal adequately with robustness issues. In particular, when the inner part, $H(s)$, of the process is subject to structural and/or parametric variations, the classical structure does not guarantee that the outer control loop can maintain acceptable performance. Measures to protect the outer loop against saturation of the inner loop are well known [2] and widely applied in practice.

This paper presents a new approach to cascade control aimed at improving control system robustness via complete decoupling of the design and performance of two (or more) cascaded control loops. The decoupling applies not only to static aspects (windup and saturations) but also to possible degradation of dynamic performance. The resulting control structure will be called the *robust structure*.

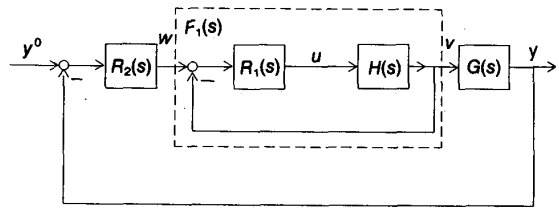

Fig. 1. Block diagram of classical structure.

Robust Design of Cascade Controllers

Assume that the plant to be controlled is composed of the series connection of the two time-invariant single-input/single-output linear systems described by the transfer functions $G(s)$ and $H(s)$ in Fig. 1.

$$Y(s) = G(s)V(s) \tag{1a}$$

$$V(s) = H(s)U(s) \tag{1b}$$

The functions $U(s)$, $Y(s)$, and $V(s)$ are the Laplace transforms of the input variable $u(t)$, the output variable $y(t)$, and the intermediate variable $v(t)$, respectively. Both variables $v(t)$ and $y(t)$ are assumed measurable.

Classical Structure

The classical structure to control the system of Eqs. (1) is illustrated in Fig. 1, where $R_1(s)$ and $R_2(s)$ are the transfer functions of the controllers. The typical procedure to design the classical structure consists of two sequential steps:

(1) Choose the controller $R_1(s)$ so that the closed-loop transfer function $F_1(s)$ has a bandwidth B_1 sufficiently larger than the bandwidth B_2, which is desired for the overall control system.

$$F_1(s) = \frac{V(s)}{W(s)} = \frac{R_1(s)H(s)}{1 + R_1(s)H(s)} \tag{2}$$

(2) Choose $R_2(s)$ according to classical design criteria for stability, performance, and robustness, under the ideal assumption that

$$F_1(s) = 1 \tag{3}$$

Step 2 of the preceding procedure can be performed by initially assigning an "ideal" value $F_{2i}(s)$ to the transfer function $F_2(s)$ between $y^0(t)$ and $y(t)$, which meets all the design specifications.

$$F_2(s) = \frac{Y(s)}{Y^0(s)} = F_{2i}(s) \tag{4}$$

Next, give $R_2(s)$ the corresponding ideal value $R_{2i}(s)$, which, in view of Eqs. (1)–(3), meets condition (4).

$$R_2(s) = R_{2i}(s) = \frac{F_{2i}(s)}{G(s)(1 - F_{2i}(s))} \tag{5}$$

Note that $R_2(s)$ is proper whenever the pole-zero difference of $F_{2i}(s)$ is chosen greater than or equal to that of $G(s)$.

Whenever Step 1 of the algorithm is not completed successfully, the validity of Eq. (3) cannot be assumed in synthesizing $R_2(s)$. A reasonable design criterion consists then of giving $R_2(s)$ the "real" value $R_{2r}(s)$, which generates a transfer function between $y^0(t)$ and $w(t)$ equal to the one produced by $R_{2i}(s)$ under assumption (3). The rationale behind this idea is that it does not make any sense to force the variable $w(t)$ in the real case more than in the ideal case, trying to speed up the slower inner loop dynamics. This, in fact, would require increasing the control effort of the outer loop, whereas it is reasonable to assume that the control effort designed for the ideal case is the maximum one permitted. This line of reasoning leads to choosing $R_{2r}(s)$ so that the transfer function $K(s) = W(s)/Y^0(s)$ remains the same as in the ideal case, i.e., $K(s) = F_{2i}(s)/G(s)$, which implies that

$$R_2(s) = R_{2r}(s) = \frac{R_{2i}(s)}{1 + R_{2i}(s)G(s)(1 - F_1(s))} \tag{6}$$

$$F_2(s) = F_{2r}(s) = F_1(s)F_{2i}(s) \tag{7}$$

Claudio Maffezzoni, Nicola Schiavoni, and Gianni Ferretti are with the Dipartimento di Elettronica, Politecnico di Milano, Piazza L. da Vinci 32, 20133 Milano, Italy.

0272-1708/90/0100-0021 $01.00 © 1990 IEEE

Robust Structure

A possible alternative to the control scheme of Fig. 1, called robust structure, is illustrated in Fig. 2. The configuration in Fig. 2 satisfies Eq. (4) provided that

$$R_3(s) = \frac{F_{2i}(s)}{G(s)} \tag{8a}$$

$$R_4(s) = F_{2i}(s) \tag{8b}$$

However, there is a basic difference between the scheme of Fig. 1 and that of Fig. 2, which renders the second scheme advantageous for practical applications. Specifically, whereas $R_{2r}(s)$ depends on $F_1(s)$ [see Eq. (6)], the transfer functions $R_3(s)$ and $R_4(s)$ depend only on $F_{2i}(s)$ and $G(s)$ [see Eqs. (8)]. In other words, the design of the pair $R_3(s)$, $R_4(s)$ is completely independent of the design of $R_1(s)$ and does not require any assumption on $F_1(s)$. This fact confers peculiar robustness properties to the robust structure. To evaluate robustness, let $F_{1p}(s)$ and $G_p(s)$ be perturbed values of the nominal transfer functions $F_1(s)$ and $G(s)$, respectively. Consider steady-state behavior and dynamic performance in the presence of model perturbations. It is easy to show that the two schemes (Figs. 1 and 2) considered are substantially equivalent at the steady state, while the situation is radically different for dynamical behavior, as shown in the following. When only function $F_1(s)$ undergoes a perturbation, we have for the classical structure with $R_2(s) = R_{2r}(s)$,

$$\frac{Y(s)}{Y^0(s)} = \frac{F_{2i}(s)F_{1p}(s)}{1 + F_{2i}(s)(F_{1p}(s) - F_1(s))} \tag{9}$$

For the robust structure, we have

$$\frac{Y(s)}{Y^0(s)} = F_{2i}(s)F_{1p}(s) \tag{10}$$

Equation (10) clearly shows that the robust structure is asymptotically stable as long as $F_{1p}(s)$ and $F_{2i}(s)$ are asymptotically stable (which is the least requirement when analyzing the outer loop robustness), whereas the same assumption does not guarantee stability of the classical structure, as is apparent from Eq. (9). When only the function $G(s)$ undergoes a perturbation, the transfer functions between $y^0(t)$ and $y(t)$ relative to the two schemes are identical. Considering now simultaneous perturbations of both functions $F_1(s)$ and $G(s)$, let $L_C(s)$ and $L_R(s)$ be the loop transfer functions for the classical structure and the robust structure, respectively; then

$$L_C(s) = L_0(s)\frac{G_p(s)}{G(s)}\frac{F_{1p}(s)}{F_1(s)}$$

with

$$L_0(s) = \frac{F_1(s)F_{2i}(s)}{1 - F_1(s)F_{2i}(s)}$$

and

$$L_R(s) = L_C(s)A(s)$$

with

$$A(s) = \frac{F_1(s)F_{2i}(s) - 1}{F_{2i}(s)F_{1p}(s) - 1} \tag{11}$$

Analytic Examples

The robustness properties of the two different control schemes may be compared by using two typical reference models. The first model is characterized by the fact that the nominal loop transfer function $L_0(s)$ is minimum phase so that, around the critical frequency ω_c, it can be written approximately as

$$L_0(s) \approx 2^{1/2}(\omega_c^2/s)/(s + \omega_c) \tag{12}$$

The second model describes the case where $L_0(s)$ is nonminimum phase and, around ω_c, can be written approximately as

$$L_0(s) \approx (\omega_c/s)\exp[-(s/\omega_c)(\pi/4)] \tag{13}$$

Observe that, for both models [Eqs. (12) and (13)], a phase margin φ_m of $\pi/4$ rad has been assumed. Now, consider phase variations in the loops

$$\frac{G_p(s)}{G(s)} = \exp(-j\varphi_G) \tag{14a}$$

$$\frac{F_{1p}(s)}{F_1(s)} = \exp(-j\varphi_F) \tag{14b}$$

$$\varphi_G + \varphi_F = \varphi_m = \pi/4 \text{ (rad) for}$$

$$\varphi_G \geq 0 \text{ and } \varphi_F \geq 0 \tag{15}$$

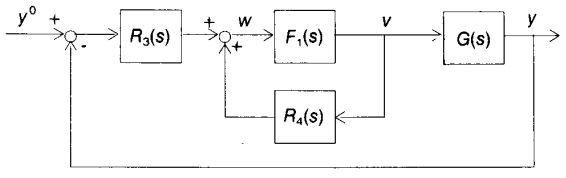

Fig. 2. Block diagram of robust structure.

Thus, the classical structure is led up to the stability limit, independently of how the total phase perturbation is split between φ_G and φ_F. It easily can be shown that, for any perturbation respecting Eq. (15), the robust structure is asymptotically stable except for the case $\varphi_F = 0$, where the two designs are equivalent by definition. To complete the analysis, the stability regions relative to the classical structure and the robust structure are also computed for gain perturbations

$$\frac{G_p(s)}{G(s)} = \mu_G$$

$$\frac{F_{1p}(s)}{F_1(s)} = \mu_F$$

In conclusion, we find that

(1) In the case of phase perturbations, the robust structure supplies a wider stability region than the classical structure.

(2) In the case of gain perturbations, the robust structure is not definitely superior to the classical structure, but exhibits a specific robustness for variations of the inner loop gain μ_F.

The results presented for the two reference models [Eqs. (12) and (13)] should not be considered as unusual, in view of the following "compensation" property of the function $A(s)$ of Eq. (11).

Property of A(s)

Let θ be the phase of the closed-loop frequency response $F_1(j\omega)F_{2i}(j\omega)$ at any frequency ω and consider any phase perturbation of the form (14) with (15). Then, for any $\theta > 0$ and $\varphi_F > 0$, the phase of $A(j\omega)$ is positive, while its magnitude is less than 1 whenever $0 < \theta < \pi$ and $0 < \varphi_F/2 < \pi - \theta$.

Illustrative Numerical Example

In order to compare the robustness of the two schemes of Figs. 1 and 2, consider the following numerical example, where $N(s)$ and $D(s)$ are polynomials of any order and $T_1 = 0.3$, $\tau_1 = 1$, and $\tau = 2$.

$$F_1(s) = \exp(-s\tau_1)/(1 + sT_1)$$

$$G(s) = \exp(-s\tau)N(s)/D(s)$$

Assume that the ideal closed-loop transfer function $F_{2i}(s)$ be chosen as follows and design the classical structure and the robust structure to have perfect equivalence in nominal conditions

$$F_{2i}(s) = \exp(-s\tau)/(1 + sT) \tag{16}$$

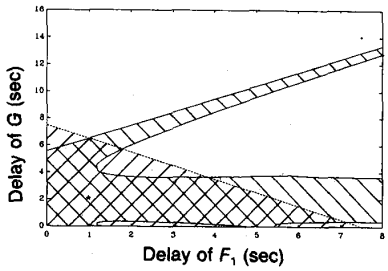

*Fig. 3. Numerical example showing stability domains with delay variations only: //////, classical structure; \\\\\\, robust structure; *, nominal conditions.*

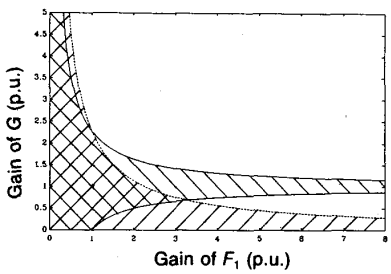

*Fig. 4. Numerical example showing stability domains with gain variation only: //////, classical structure; \\\\\\, robust structure; *, nominal conditions.*

where $T = 1$. Then consider the following perturbed transfer functions:

$$F_{1p}(s) = \mu_1 \exp(-s\tau_{1p})/(1 + sT_1);$$

$$\mu_1 > 0, \tau_{1p} > 0$$

$$G_p(s) = \mu \exp(-s\tau_p)N(s)/D(s);$$

$$\mu > 0, \tau_p > 0$$

The robustness analysis is synthesized by the stability regions of Figs. 3 and 4, where the two couples of parameters (τ_{1p}, τ_p) and (μ_1, μ) are varied separately. They confirm that the new design is definitely superior when the parameter perturbations do affect $F_1(s)$.

Application to Steam Temperature Control

The application of the new concept to superheated steam temperature control in a natural-circulation oil-fired drum boiler is considered here. A complete "first-principle" modular model is set up using the computer-aided modular modeling and simulation code, LEGO, presented in previous papers (e.g., [3] and [4]). The resulting model, referred to here as the reference model, is a nonlinear, large-scale dynamic system consisting of 84 differential equations and 160 algebraic equations describing the energy, mass, and momentum balance in the various boiler subsystems. The validation of the model with respect to experimental plant tests is reported in [5]. The conceptual scheme of the classical structure for the steam temperature control [6] is shown in Fig. 5.

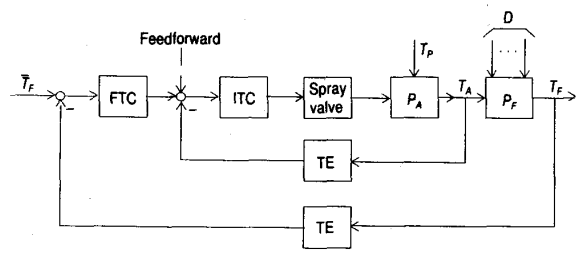

Fig. 5. Block diagram of superheated steam temperature control.

FTC = final temperature controller
ITC = intermediate temperature controller
TE = temperature measurement element
P_A = desuperheating process
P_F = final superheating process
T_F = final steam temperature
$\bar{T}_F$ = set point for T_F
T_A = final superheater inlet steam temperature
T_P = primary superheater outlet steam temperature
D = disturbance inputs for the final superheater

To obtain a transfer-function model suitable for control design, step variations of the control variable (the spray valve position) have been applied to the reference model at different plant loads, removing the dynamics of the actuator only for the identification tests. Since a gain scheduling technique is used to track the load-dependent process parameter variations, we will henceforth consider only the operating point affected by the worst dynamics, i.e., the minimum control load (40 percent of the nominal load for the plant considered). Two different linearized models have been fitted to the second part of the plant transfer function P_F: the first consisting of a dead time plus a time constant, and the second consisting of a dead time plus a double pole. The results of the fit are illustrated in Fig. 6, where the linear model responses are compared with the reference model response, with the transfer-function parameters given in the Table.

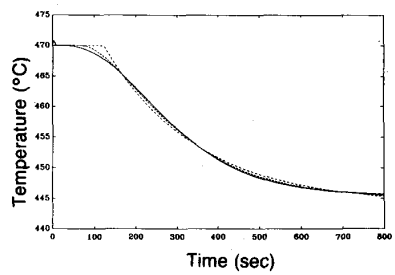

Fig. 6. Best-fit results for transfer function P_F: —, reference model; – – –, accurate model; – · –, simplest model.

For the first part of the process P_A, a simple gain μ_A can be taken as a good approximation for the sake of control design (from the reference model fit, $\mu_A = 146.6$ is obtained in units of °C/p.u. of spray valve area). The feedback control temperature element (TE) has been modeled by a lag element with time constant $T_E = 50$ sec at 40 percent load, while the valve actuator has been described by a limited rate lag element with a time constant $T_C = 5$ sec for small variations and a total traveling time of 20 sec.

The design of the superheated steam temperature control according to the classical structure (Fig. 5) assumes for inner loop forward control intermediate temperature control (ITC) a proportional-integral (PI) controller and for final temperature control (FTC) a proportional-integral-derivative (PID) controller; in the linearized framework, the scheme of Fig. 5 can be given the form of Fig. 1 with $G(s)$ given by the Table and

$$H(s) = \mu_A/[(1 + sT_C)(1 + sT_E)]$$

Table
Linear Approximations of Process Part P_F

Model	Transfer Function $G(s)$	Gain	Dead Time, sec	Lag, sec
Simplest	$\frac{\mu_F \exp(-s\tau_F)}{1 + sT_F}$	1.42	121.8	226.36
Accurate	$\frac{\mu'_F \exp(-s\tau'_F)}{(1 + sT'_F)^2}$	1.36	68.2	124.7

Parameter tuning of the PI part of the ITC inner loop controller is straightforward and was performed to yield the following nominal closed-loop transfer function

$$F_1(s) = 1/(1 + 2sT_C)^2$$

where $T_C = 5$ sec.

Considering that the dynamics of $F_1(s)$ are very fast, the synthesis of the PID controller of the outer loop has been obtained to ensure a phase margin of $\pi/4$ rad. For the design of the robust structure (Fig. 2), the ideal value $F_{2i}(s)$ of the closed-loop transfer function $F_2(s)$, defined earlier, has been chosen to obtain the same speed of response as for the classical structure in nominal conditions, when using the accurate model or the simplest model, respectively (see Table):

$$F_{2i}(s) = \exp(-s\tau'_F)/(1 + 20s)^2$$

or

$$F_{2i}(s) = \exp(-s\tau_F)/(1 + 40s)$$

To test control robustness, the performance variations of the classical structure and the robust structure have been compared for a number of process-model discrepancies.

(a) Use of the simplest model instead of the accurate one

(b) Wrong evaluation of the feedback TE lag, assuming a real lag of 100 sec instead of the nominal value of 50 sec

(c) 30 percent variation of the heat-transfer factor for the final superheater

(d) Rate saturation of the valve actuator

(e) 50 percent reduction of the spray valve gain (due to reduction of the valve differential pressure and/or valve nonlinearities)

The comparison tests have been carried out by applying the different controllers to the reference model of the steam generator, where a turbine throttle step variation of 5 percent was simulated for tests a, b, c, and e, whereas a temperature set point of 12°C was simulated for test d. The results can be summarized as follows (Fig. 7):

(1) The performances of the classical structure and the robust structure are, by design, substantially equivalent in nominal conditions (i.e., when using the accurate design model).

(2) In cases b, c, and d, the performance degradation is very similar for the two control structures considered and, in any case, quite tolerable; therefore, the corresponding simulation tests are not given here.

(3) In case a, where part P_F of the process is affected by model errors, the maximum transient temperature error is nearly equal for the two control structures, while the classical structure exhibits a more significant damping reduction.

(4) In case e, where part P_A of the process is affected by parameter variations, the behavior of the two considered controllers is rather different: the response of the robust structure becomes a bit slower, as the valve gain reduction slows down the inner loop response; the response of the classical structure becomes more oscillatory, because it undergoes a phase margin reduction when the inner loop lags increase.

Again, we have found that the robust structure exhibits enhanced robustness with respect to inner loop response changes, which do not significantly affect its stability degree or damping.

A further important robustness property of the proposed robust structure is that the outer regulator is intrinsically free from windup, because transfer function $R_3(s)$ of Fig. 2 generally does not incorporate any integral action; this greatly simplifies the overall control logic, as the only measure required to prevent windup is the usual saturation of the valve controller.

Conclusions

With the aim of devising a new control concept, combining good performance in nominal conditions with enhanced robustness to process parameter variations, a cascade control structure has been proposed, endowed with the following basic properties:

(1) Independent design of cascaded control loops;

(2) Ability to make outer loop stability (and response) independent of the possible parameter variations affecting the inner loops;

(3) Intrinsic avoidance of windup problems for the upstream controllers in the cascade; and

(4) Robustness with respect to single-loop model errors comparable with classical design (e.g., PID control).

In addition to these basic properties, we have shown in the application that the complexity of the resulting controller is comparable with that of classical cascade controllers. Finally, it is worth noting that the design method can be applied directly to deal with any number of nested cascaded control loops.

Acknowledgment

This paper has been partially supported by MPI and CNR, Centro di Teoria dei Sistemi.

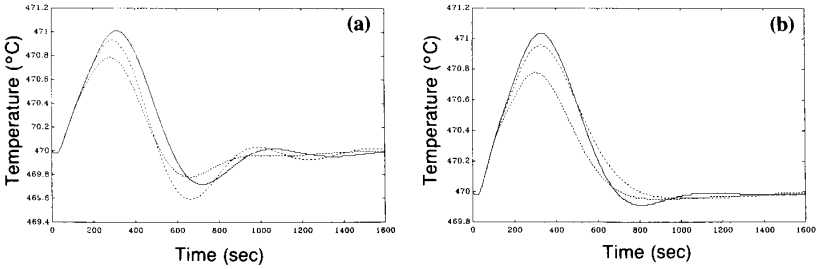

Fig. 7. Steam temperature control: (a) classical structure; (b) robust structure. (– – –, accurate model with nominal parameter values; —, simplest model; – · –, spray gain variation.)

References

[1] P. Harriott, *Process Control*, New York: McGraw-Hill, 1964.

[2] F. G. Shinskey, "Controlling Multivariable Processes," Instrument Society of America, Triangle Research Part, N.C. 1981.

[3] L. Marcocci and S. Spelta, "Computer-Aided Modelling of Complex Processes: A Program Package," *Proc. IMACS Intl. Symp. Sim. Eng. Sci.*, pp. 9–14, Nantes, France, 1983.

[4] C. Maffezzoni, G. Magnani, and L. Marcocci, "Computer-Aided Modelling of Large Power Plants," *Proc. IFAC Workshop on Modelling and Control of Electric Power Plants*, pp. 1–9, Pergamon Press, 1984.

[5] M. Adinolfi and G. Ferretti, "Simulation and Control of a Natural-Circulation Steam Generator," Thesis, Politecnico di Milano, Italy, 1987 (in Italian).

[6] P. S. Buckley, *Techniques of Process Control*, Wiley, New York, 1964.

Claudio Maffezzoni was born in Cremona, Italy, in 1946, and received the "Laurea" degree in electrical engineering from the Politecnico di Milano in 1970. He was with the Department of Electronics of the Politecnico di Milano from 1970 to 1974, and then worked for the Italian Electricity Board (Research & Studies Division) from 1974 to 1985. Since 1985, he has been with the Politecnico di Milano, where he presently holds the position of Full Professor of Process Control. He was a Vice Chairman of the IFAC Application Committee as the convener of the Working Group on Electric Generating Plants. His principal research interests are energy process control and simulation and computer-aided control engineering.

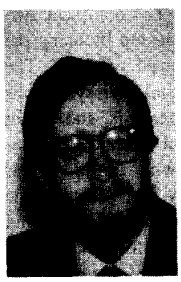

Nicola Schiavoni was born in Manduria, Italy, in 1950, and received the "Laurea" degree in electrical engineering from the Politecnico di Milano in 1973. Since then he has been with the Centro di Teoria dei Sistemi of the CNR, the Italian National Research Council, and the Politecnico di Milano, where he presently holds the position of Associate Professor of Automatic Control. His research activity has focused on various fields of system and control theory and currently specifically concerns multivariable systems and digital control. The results achieved are witnessed by about 40 articles, conference papers, and technical reports. He also has spent periods of research with the Department of Mechanical Engineering, University of California, Berkeley, and the Control and Management Systems Division, University of Cambridge, Cambridge, United Kingdom.

Gianni Ferretti was born in Cremona, Italy, in 1962, and received the "Laurea" degree in electrical engineering in 1987 from the Politecnico di Milano, where he presently holds the position of Ph.D. student. His principal research interests are computer-aided control engineering and simulation and control of mechanical systems.

1990 ACC

The American Automatic Control Council will hold the ninth American Control Conference (ACC) Wednesday through Friday, May 23–25, 1990, at the Sheraton Harbor Island Hotel, San Diego, California. This conference will bring together people working in the fields of control, automation, and related areas.

Both contributed and invited papers will be included in the program. The ACC will cover a range of topics relevant to the theory and practical implementation of control and industrial automation and to university education in controls. Topics of interest include, but are not limited to, the following: linear and nonlinear systems, identification and estimation, signal processing, multivariable systems, large-scale systems, robotics and manufacturing systems, guidance and control, sensors, simulation, adaptive control, optimal control, expert systems, and control applications.

The Organizing Committee plans to arrange workshops to be held in conjunction with the 1990 ACC.

For further information, contact the General Chairman:

Dagfinn Gangsaas
Boeing Advanced Systems
P.O. Box 3707, M/S 33-12
Seattle, WA 98124-2207
Phone: (206) 241-4348

A series of islands, lagoons, waterways, and peninsulas form this 4600-acre public recreational complex located within the city of San Diego. As the largest aquatic park in the world, it offers visitors a year-round melange of water activities in addition to the many scenic parks and beaches, fine restaurants, exciting nightlife, and elegant hotels.